UC-34A
LBL-20834
c.1

Lawrence Berkeley Laboratory

UNIVERSITY OF CALIFORNIA

RECEIVED
LAWRENCE
BERKELEY LABORATORY
MAR 6 1986
LIBRARY AND
DOCUMENTS SECTION

Accelerator & Fusion Research Division

Presented at the Synchrotron Radiation Sources
and Their Applications Conference,
Aberdeen, Scotland, September 14-18, 1985

MIRROR SYSTEMS

M.R. Howells

December 1985

For Reference

Not to be taken from this room

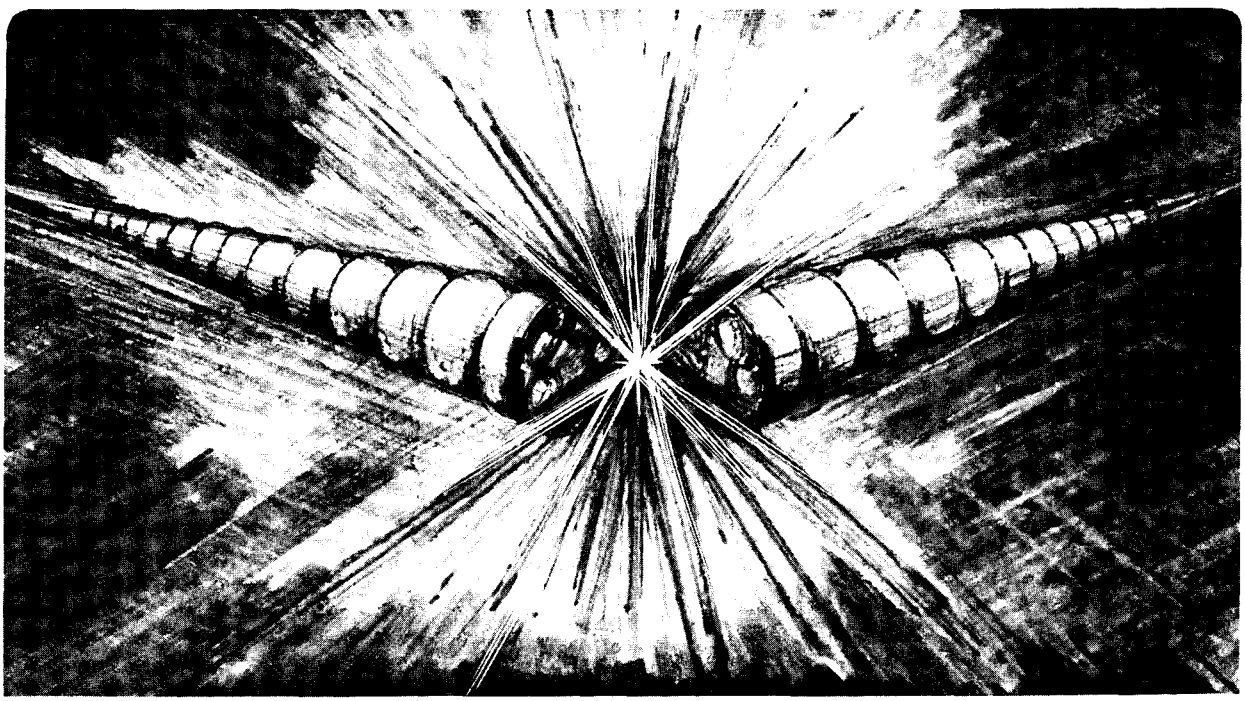

LBL-20834
c.1

Prepared for the U.S. Department of Energy under Contract DE-AC03-76SF00098

DISCLAIMER

This document was prepared as an account of work sponsored by the United States Government. While this document is believed to contain correct information, neither the United States Government nor any agency thereof, nor the Regents of the University of California, nor any of their employees, makes any warranty, express or implied, or assumes any legal responsibility for the accuracy, completeness, or usefulness of any information, apparatus, product, or process disclosed, or represents that its use would not infringe privately owned rights. Reference herein to any specific commercial product, process, or service by its trade name, trademark, manufacturer, or otherwise, does not necessarily constitute or imply its endorsement, recommendation, or favoring by the United States Government or any agency thereof, or the Regents of the University of California. The views and opinions of authors expressed herein do not necessarily state or reflect those of the United States Government or any agency thereof or the Regents of the University of California.

LBL-20834

MIRROR SYSTEMS

M.R. Howells

Lawrence Berkeley Laboratory
University of California
Berkeley, California 94720

December 1985

This work was supported by the U.S. Department of Energy under Contract Number DE-AC03-76SF00098.

MIRROR SYSTEMS

LECTURE 2:

Malcolm R. Howells
Center for X-ray Optics, Lawrence Berkeley Laboratory
1 Cyclotron Road, Berkeley, California 94720

1. INTRODUCTION

Mirrors have been the most important optical components for beam transport functions since the earliest days of the application of synchrotron radiation to spectroscopy. Originally they were made in the same way that mirrors were made for visible light applications, using a glass or fused silica substrate. With a gold or platinum coating and a suitable choice of grazing angle such mirrors gave satisfactory service as relay optics in the first generation of synchrotron radiation beamlines.

As the technology of synchrotron radiation exploitation has become more sophisticated a number of developments have occurred which place increased demands on the performance of mirrors and it has become apparent in recent years that mirror performance must be included as a primary design factor in beamline planning. Modern synchrotron radiation sources particularly wigglers and undulators have much higher brightness than earlier ones. For the optical designer this brings the double challenge of requiring more precise focussing to be achieved in the presence of much higher photon beam power. In addition, modern sources are dedicated storage rings so one must also try to collect the largest possible solid angle by placing mirrors near the source and in its ultra high vacuum environment.

The issues raised by these developments have been reviewed by various authors especially Rehn and co-workers[1-4], Johnson[5], Howells[6] and Saille[7]. In addition there have been three workshops[8] and several conferences[9] containing material on the subject. Beside the

efforts of synchrotron radiation scientists there have been parallel attempts by workers in x-ray astronomy[10-13], high power laser technology[14,15] and plasma diagnostics[16] to improve the performance of optical reflecting surfaces operating in hostile environments.

Although a great deal of progress has been made in improving optical components, we must say that at the present time they are not keeping pace with the increases in demand which in certain cases are approaching the ultimate which is the diffraction limit. The only types of surface which can presently be specified with real confidence that the desired surface quality will be achieved are flats and spheres. All other, more complex surfaces, have the potential for being a limitation on beamline performance. For these reasons, future beamlines are likely to show a reversion to earlier practice which was to depend heavily on spherical and flat surfaces especially for resolution-determining optics.

In this article we do not have space to discuss sophisticated modern developments in detail. Therefore we choose to concentrate on basic material with extensive references to the recent applications.

2. THE REFLECTION PROCESS

The physics of VUV and x-ray reflection is the same as that of visible light and is fully covered by classical electromagnetic theory provided the refractive index of the reflector is specified. The main difference in practice is caused by the fact that the real part of the refractive index is usually less than unity so that total reflection at a vacuum/material interface takes place on the vacuum side. In addition absorption is almost always important so the refractive indices and reflection and transmission coefficients for the wave <u>amplitude</u> are complex. The most useful treatment of this process for us is that of Born and Wolf[17]. We summarise the conclusions of these authors below.

Consider an infinite plane wave of unit amplitude incident at angle θ to the normal of an infinite plane interface between vacuum and a material of refractive index $\tilde{n} = n - ik$. Suppose the electric vector of the wave is perpendicular to the plane of incidence i.e. we consider s (that is σ) polarisation and further, suppose the

reflected amplitude r_s is given by

$$r_s = \rho_s e^{i\phi_s} \tag{1}$$

so that ϕ_s is the phase change on reflection. Then using $|r_s|^2 = R_s$ we have

$$R_s = |\rho_s|^2 = \frac{(\cos\theta - u)^2 + v^2}{(\cos\theta + u)^2 + v^2} \tag{2}$$

$$\tan\phi_s = \frac{2v\cos\theta}{u^2+v^2-\cos^2\theta} \tag{3}$$

$$u = \frac{1}{\sqrt{2}}\left[Q + \sqrt{Q^2+4n^2k^2}\right]^{\frac{1}{2}} \tag{4}$$

$$v = \frac{-1}{\sqrt{2}}\left[Q - \sqrt{Q^2+4n^2k^2}\right]^{\frac{1}{2}} \tag{5}$$

and

$$Q = n^2 - k^2 - \sin^2\theta \tag{6}$$

Similarly for p (that is π) polarisation we get

$$R_p = |\rho_p|^2 = \frac{[(n^2-k^2)\cos\theta - u]^2 + [2nk\cos\theta + v]^2}{[(n^2+k^2)\cos\theta + u] + [2nk\cos\theta - v]^2} \tag{7}$$

$$\tan\phi_p = \frac{2knu + (n^2-k^2)v}{(u^2+v^2) - (n^2+k^2)^2\cos^2\theta} \tag{8}$$

There are also four corresponding equations for the transmitted amplitudes.[18] These can be up to twice the incident amplitude leading to a maximum for the transmitted intensity of four times incident. In the direction perpendicular to the interface the transmitted intensity decays exponentially with distance with 1/e penetration $Z_{1/e}$ given by

$$Z_{1/e} = \frac{\lambda}{4\pi v} \tag{9}$$

where λ is the wavelength.

To illustrate the reflection process we show in fig. 1 the intensity reflectance, intensity transmittance and the phase change on reflection for nickel for four wavelengths ranging from the x-ray to the VUV. Visible differences between s and p polarisation only appear for the longest of the four wavelengths. In fig. 2 we show the reflectance of nickel in the soft x-ray region according to Henke.[19] We note the bad effect of the nickel $L_{II,III}$ edges around 860eV.

Allowing for practical matters such as ease of deposition, chemical stability plus the reflectance characteristics, a relatively small

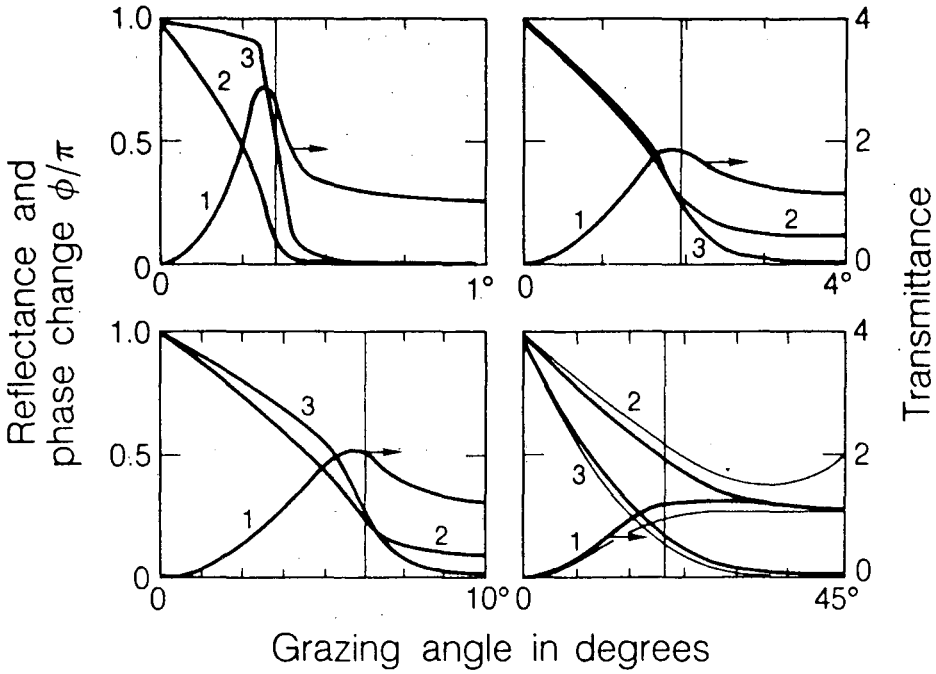

XBL 8512-12837

Fig 1. Curves of transmittance (1), phase change on reflection (2) and reflectance (3) for nickel as a function of grazing angle. The vertical line indicates the critical angle. The graphs refer to the following wavelengths and refractive indices (top left) 1.5Å($\tilde{n}$=0.99982-i0.00000050), (top right) 8.34Å($\tilde{n}$=0.99941-i0.00059), (bottom left) λ=31.4Å($\tilde{n}$=0.994-i0.0015, and (bottom right) λ=137Å($\tilde{n}$=0.94-i0.06). Differences between s and p polarisation are discernable only for λ = 137Å

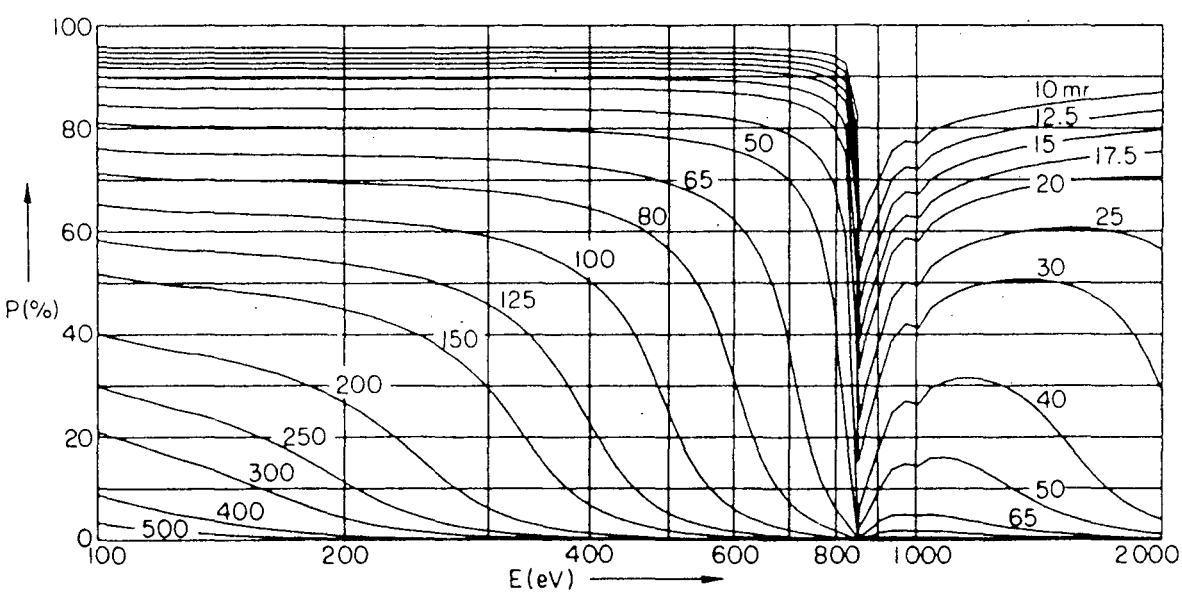

XBL 8512-5129

Fig 2. Reflectance curves for nickel as given by Henke (reference 19) for the soft x-ray region.

number of materials have become important as reflective coatings for mirrors. For our purposes the important ones are:

Near UV	< 10eV	MgF_2 coated Al, Au
VUV	10-100eV	Au, Pt, Os, SiC*,
Soft x-ray	100-3000eV	Au, Pt, Ni, Cr, Rh,
X-ray	3000-20,000eV	Au, Pt, Ni, Rh,

*Silicon carbide[20] would be used as substrate as well as the reflecting surface.

3. MIRROR FUNCTIONS ON SYNCHROTRON BEAMLINES

The main functions of mirrors in synchrotron beamlines are as follows:

(i) Deflection: achieves separation of different beamlines derived from the same port, allows manipulation of floor space occupancy.

(ii) Filtration: for a given incidence angle higher photon energies are absorbed, lower ones reflected. This is based on the existence of a critical angle at each energy (see fig 1). The cut off occurs roughly when $\sin\theta \sim n$ where n is a function of photon energy.

(iii) Power absorption: specially designed water cooled power absorbing mirrors (which are generally expensive and are preferably not resolution-determining) can be used to protect more fragile uncooled optical systems which may be resolution-determining. This is particularly necessary if VUV/soft x-ray experiments must be done using a source with a large hard x-ray output.

(iv) Condensation: i.e. forming a real image of the source (or a real image of a real image of it). Condensing mirrors relay light from the source to the entrance slit of a monochromator or from the exit slit of a monochromator to a sample. They are not resolution determining.

(v) Focusing: for plane grating monochromators there must be a "camera" mirror which focuses the angularly dispersed light from the grating into the exit slit plane. For imaging systems (reflection microscopes or microprobes) one again has mirrors which focus to the focal plane of the system. In both these cases the wavelength (or spatial) resolution of the device <u>is</u> determined by the image quality of the mirror.

(vi) Collimation: i.e. rendering divergent light parallel. This is desirable when the divergence angle of synchrotron radiation is greater than the rocking curve width of a monochromator crystal or to give parallel light to illuminate a plane grating. Either way the collimator is resolution-determining.

All mirrors carry out more than one of these functions and the designers task is to achieve the desired result as simply as possible.

In many of the functions one would like to achieve point to point imaging (either or both points could be at infinity). To accomplish this we recognise that ellipsoids and paraboloids of revolution can, in theory, image a single point (the axial point) perfectly for any chosen grazing angle. Other points are imaged with aberrations but, in practice, for cases other than the x-ray microscope, the aberrations are usually negligible and one would be very happy to use an ideal ellipsoid or paraboloid of revolution. However, these surfaces are very difficult to make with sufficiently perfect figure and finish and to get better tolerances (and equivalently, lower prices) one becomes interested in surfaces which approximate ellipsoids or paraboloids of revolution but which are easier to make. The most important of these is the "bicycle tyre toroid". Another important strategy is to use two focusing mirrors to separately focus in the horizontal and vertical directions in the manner of the Kirkpatrick-Baez X-ray Microscope. This has the advantage that the horizontal and vertical magnifications can be chosen independantly and that the reflecting surfaces can be spherical. This type of design is likely to be used in the future because the extreme tolerances that will be needed may be achievable only on spherical surfaces.

4. METHODS OF FABRICATION

The traditional method of fabrication of optical surfaces which has been used in various forms for centuries is still the most important one for synchrotron radiation beamlines. The method is based on the ability of a polishing slurry and a soft tool made of pitch moving with a pseudo-random motion to apply a sort of averaging process to an initially approximately spherical surface. The effect is that the surface becomes more and more exactly spherical. This works well for

flat and spherical surfaces and can, in the right hands give good results[22] for all the important substrate materials i.e. glass, fused silica, silicon carbide, copper, aluminum, molybdenum, beryllium (and their alloys) and electroless nickel. The latter is a chemically coated form of amorphous nickel which is usually applied as a coating about .05-.5 mm thick. A variant on the above process known as "super-polishing"[21] must be applied in order to get the high quality finish needed for synchrotron radiation optics and this works well only for glass, fused silica, silicon carbide and electroless nickel out of those listed above. This is the reason why metal mirrors are usually coated with electroless nickel.

In order to get final correction of spherical surfaces or to make aspheric surfaces it is necessary for a craftsman to utilize a measurement, correction loop to achieve a specified surface figure. The traditional methods of visible light interferometry[23] supply the needed measurement step in this process. However, these methods tend to fail as one moves from normal incidence toward grazing incidence and consequently both manufacture and inspection of grazing incidence optics has always been a somewhat inaccurate business.[24] This has often not mattered or not been discovered since the customer usually had even less measurement ability than the fabricator. However for planned synchrotron light sources one would like to have surfaces of 1-10 μradian accuracy. This is fairly standard for spherical optics[25] but not yet attained for grazing incidence aspherics. The better manufacturers can achieve tolerances in the range 10-100 μradian. Toroids tend to be better than conics and smaller optics better than larger.

Another approach to fabricating difficult grazing incidence surfaces is to buy a cylindrically surfaced mirror and bend it[26] to get a toroidal or similar surface. This is often done mainly to save money (which it generally does not) and its impact on surface tolerances is usually not determined. The approach does give some control over the mirror surface and with enough degrees of freedom one could probably achieve better tolerances than with a rigid mirror. However such "adaptive optics"[27] methods are used in various astronomical and

military applications and are known to produce good tolerances only at very high cost.

5. TYPES OF IMPERFECTION

5.1 Aberrations

Even a perfect mirror produces an aberrated image except, perhaps, for a single point in the object field. The effect of aberrations can be studied either analytically by calculating the optical path function, as is done for diffraction gratings[5,28] (mirrors are a special case of gratings) or by exact ray tracing.[29] One cannot do serious beamline design without a good ray trace program but it must be noted that such programs do not invent beamline designs. They merely evaluate them.

5.2 Surface figure inaccuracy

Departures from the ideal surface are usually divided into those with a transverse width scale greater than about 1mm and those which are smaller than that. The larger ones can often be measured by interferometry and are called "figure errors" and the smaller must be measured differently (see next section) and are called "roughness". In either case the first step for the designer is to establish tolerances which will guarantee proper function. The art is to conceive a system which uses realistic materials and fabrication methods and has tolerances which are not only achievable in practice but which can be achieved and verified within the available budget. The practical limitations on mirror choices and tolerances turn out to be one of the primary factors determining the type of beamline one chooses to build.

The way to establish tolerances is to think in terms of geometrical rays and consider each element of the mirror as a "ray steering" device. For mirrors which image the source the effect of a slope error on the mirror is a shift in the apparent point of origin of a ray in the source plane relative to its actual point of origin. For example if we take a shift of a quarter of the source width as tolerable then the mirror surface slope tolerance in the plane of incidence would be an eighth of the angular subtense of the source at

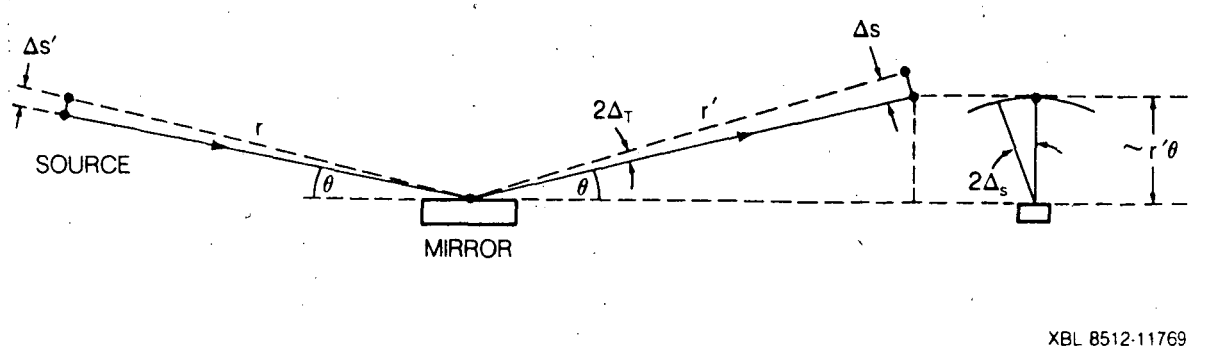

Fig 3. Mirror surface tolerances: suppose there are slope errors Δ_T in the plane of incidence and Δ_S in the sagittal plane. Apparently $2\Delta_T \simeq \Delta s'/r' = \Delta s/r$ as explained in the text. For the sagittal plane (right hand picture) $2\Delta_S \simeq \Delta s'/r'\theta = \Delta s/r\theta$ which is larger by a factor θ^{-1}

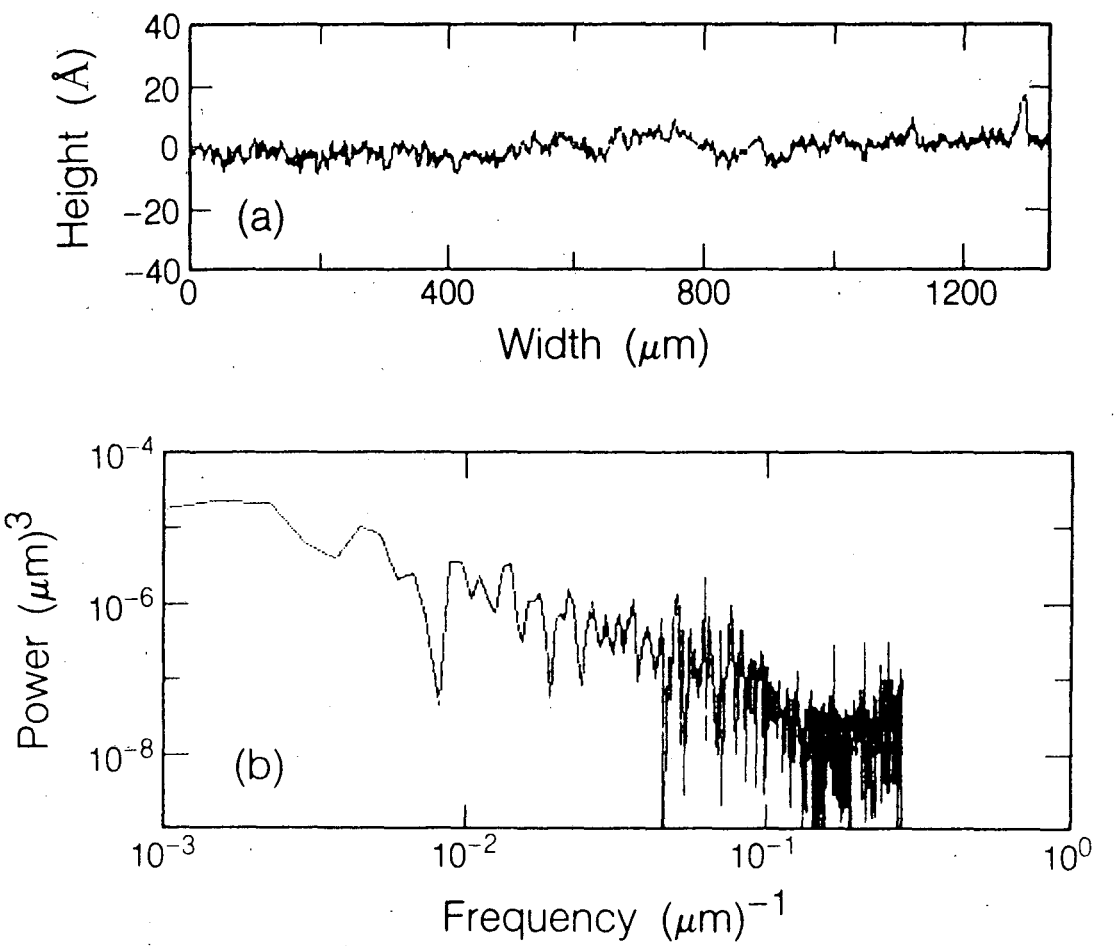

Fig 4. Surface profile and power spectrum for a good quality glass surface. The finish parameters are given in the text for various bandwidths

the mirror in that plane. This can be a sub arc second tolerance but if it is not achieved the effective source size will increase which is equivalent to a loss of brightness. However, it is important to note that in the plane perpendicular to the plane of incidence the tolerances are larger (easier) by a factor of one over the grazing angle. This is explained in fig. 3. The effect is that the transverse tolerances are usually very easy and for the important class of vertically reflecting x-ray mirrors we must consider the mirrors to be always perfect in the horizontal plane.

5.3 Roughness

With present day instrumentation[30] it is possible to trace out the surface profile of a mirror over about a 1mm scan with height resolution less than 5Å and resolution parallel to the scan of about 1μm. This surface profile is a sample function of a random process which gives a description of the quality of the surface finish of the mirror and can be used to predict the amount and angular distribution of the scattered light.[31] The latter can, in bad cases, lead to serious blurring of the ideal image. In order to get a parameter that attempts to characterise the surface finish one can compute the r.m.s. height (σ) of the surface profile. However this parameter is not simply related to the function of the mirror because of bandwidth[32] effects. We should consider the surface roughness to be a Fourier superposition of many different spatial frequencies each of which is visualised as a sinusoidal diffraction grating. The highest frequency gratings give the largest scattering angles as determined by the grating equation. Now in any application there will be a low frequency limit f_{min} which causes such small scattering angles that they are indistinguishable from perfect performance. Similarly there will be a high frequency limit f_{max} Now unless the profile was measured with the bandwidth limits f_{min} and f_{max} appropriate to the application the r.m.s. profile height will not be a useful indicator of performance. One can readily show this by computing σ values with different bandwidth limits from the same data set.[33] One often gets orders of magnitude change for different choices of f_{min} and f_{max}. Thus σ values quoted as appropriate for visible light

optical system performance and measured by visible light scattering often have the wrong bandwidth limits to be a valid indicator of x-ray performance. The spatial wavelengths that must be included for x-ray work that are usually not included in visible light work are roughly those in the region 10-1000μm (sometimes called "ripple").

This is all most unfortunate because visible light scattering is the only easy and cheap method of surface finish measurement. However now that instrumentation for measuring surface profiles with a sufficiently wide bandwidth for most x-ray work can be bought commercially[34] we can expect to see gradual improvement in techniques for polishing x-ray optical surfaces and the development of a rational basis for specifying and inspecting surface finish. The surface shown in fig. 4[35] is a good one and has σ values as follows

$f_{min}(\mu m)^{-1}$	$f_{max}(\mu m)^{-1}$	σ(Å)	m(mrad)	
.083	.286	0.9	.104	(high frequency)
.0008	.082	3.2	.048	(low frequency)
.0008	.286	3.4	.115	(profilometer limited)

About 10Å is a reasonable choice at the present time for a wide band σ value that can be achieved. However, we cannot predict performance quantitatively without at least one more parameter. Ultimately, what we would like to know is the r.m.s. angular width of the scattering distribution (Δθ) which is given by

$$\Delta\theta = \frac{m\lambda}{2\pi\sigma}$$

where m is the r.m.s. slope and λ refers to the photons. The parameter m is derivable from the profile.[36]

5.4 Degradation due to use

The main degradation of beamline optical surfaces is due to contamination by a carbonaceous[37] overlayer. This gives lower reflecting efficiencies and unwanted structure in the wavelength dependance of the reflectance. There is also evidence that there is a certain amount of roughening.[39] The contamination rate[38] is determined by the rate of emission of photoelectrons (and hence by the incident flux) and the partial pressure of whichever carbon containing molecules are responsible. The only full solution is to remove the carbon layer

either by wet chemistry for mirrors made from chemically inert substrates such as fused silica or silicon carbide or else by oxidation by oxygen atoms in an R.F. discharge.[40,41] Partial solutions are to recoat the surface over the top of the carbon layer (possibly in situ) or to use large optical surfaces with several working areas.

Other forms of degradation have been observed including both reversible and irreversible swelling due to non-thermal damage by ionising radiation.[42] This is particularly problematical with fused silica and zerodur mirrors. The most important threat of permanent damage to mirrors, however, is due to photon beam thermal loading and to this we now turn.

6. PHOTON BEAM THERMAL LOADING

6.1 Calculating the Thermal load

The power and power density in a synchrotron radiation beam can be calculated by integrating the synchrotron radiation spectrum over frequency. This has been done for the general case only rather recently by K.J. Kim[43] whose results we summarise below. Consider an undulator with maximum angular deflection K/γ where γ is the electron beam energy in units of the electron rest energy. Let B_o be the peak magnetic field, λ_o the period, I the electron current, N the number of periods and P_T the total output power. Then

$$P_T = \frac{\pi N Z_o I e c \gamma^2 K^2}{3\lambda_o}$$

Where Z_o = 377 ohms, the impedance of free space, e is the electronic charge and c the velocity of light.

In practical units

$$P_T = 0.633\ E^2(\mathrm{GeV})\ L(\mathrm{m})\ I(\mathrm{A})\ B_o^2(\mathrm{T})\ \mathrm{kW}$$

The on-axis power density is given by

$$\left.\frac{dP}{d\Omega}\right|_{\substack{\text{on}\\ \text{axis}}} = \frac{21}{4\pi}\ \frac{P_T}{\frac{2}{\gamma}\cdot\frac{2K}{\gamma}}\ G(K)$$

where $$G(K) = K\left[\frac{K^6+\frac{24}{7}K^4+4K^2+\frac{16}{7}}{(1+K^2)^{7/2}}\right]$$

or in practical units

$$\left.\frac{dP}{d\Omega}\right|_{\substack{\text{on}\\ \text{axis}}} = 10.84\ B_o(\mathrm{T})\ E^4(\mathrm{GeV})\ I(\mathrm{A})\ N\ G(K)\ \mathrm{W/mr^2}$$

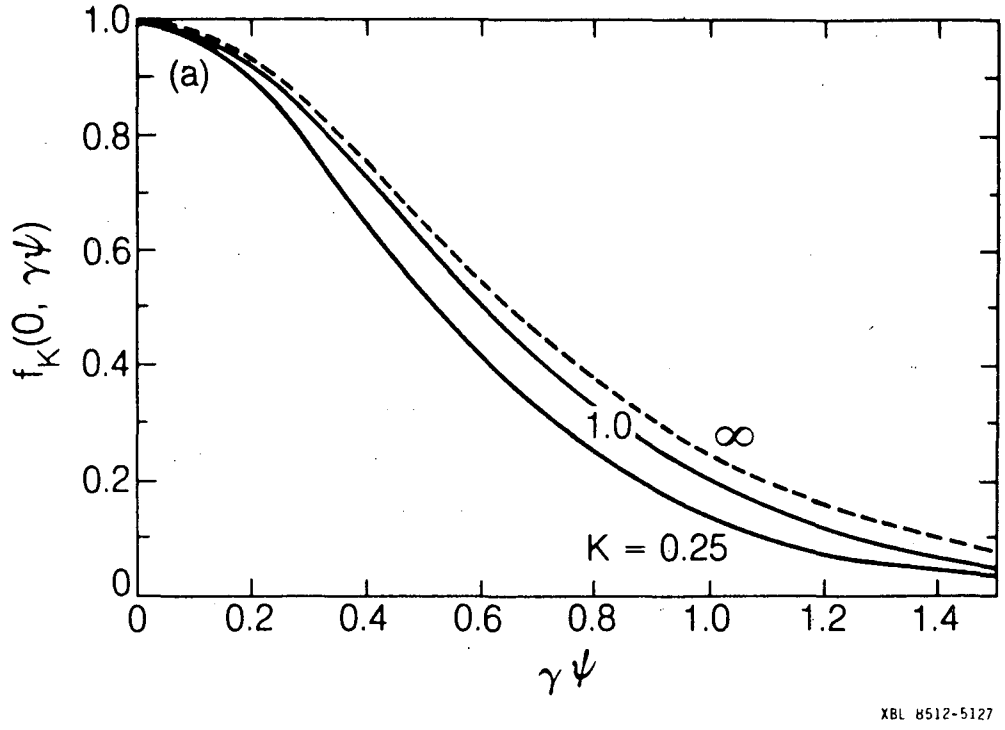

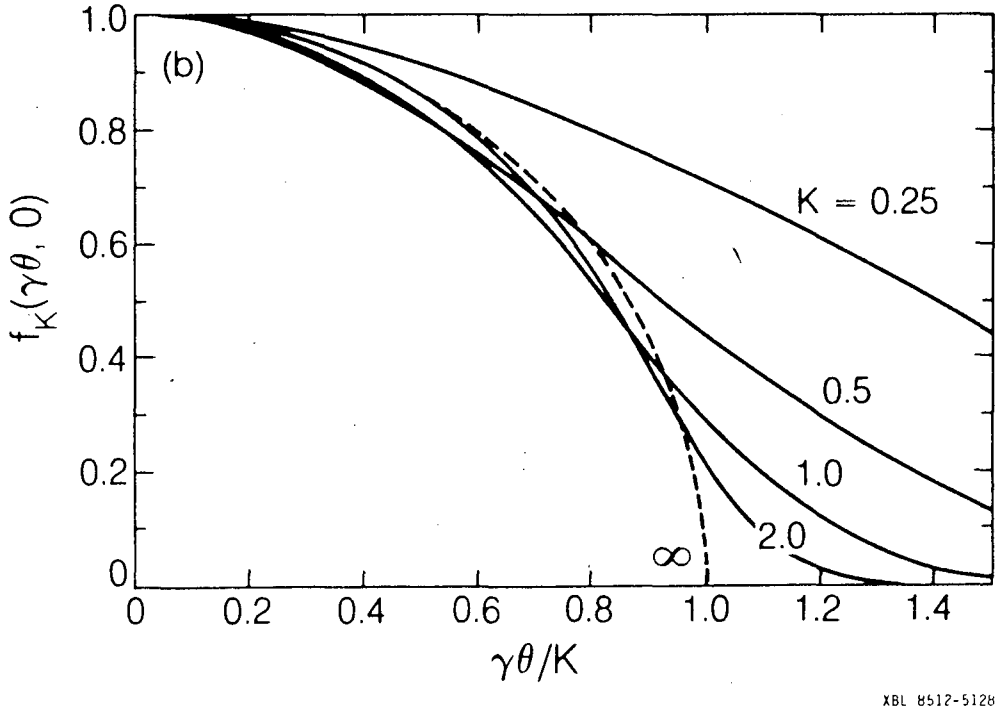

Fig 5. $f_K(0,\gamma\psi)$ and $f_K(\gamma\theta,0)$ from reference 43

Notice that $G(K)\to 1$ as K becomes larger than about unity. Kim also gives the angular distributions in the form

$$\frac{d^2P}{d\theta d\psi} = \frac{dP}{d\Omega}\bigg|_{\substack{\text{on}\\ \text{axis}}} f_K(\gamma\theta,\gamma\psi)$$

where θ is the horizontal angle and ψ the vertical and $f_K(0,0)=1$. Fig. 5 shows $f_K(0,\gamma\psi)$ and $f_K(\gamma\theta,0)$ for various values of K. The vertical distribution is fairly well approximated[44] by a Gaussian with standard deviation $0.61/\gamma$.

6.2 General Principles[50]

There is no single, typical geometry in which synchrotron radiation falls on mirror surfaces but the use of small grazing angles tends to give a "footprint" in the shape of a narrow line. Consider a line of length L and width W of power input to a surface and suppose cooling is at a distance R>>W. Then for a material with conductivity k we might assume cylindrical heat flow and get for the temperature rise ΔT

$$\Delta T = \frac{Q \log_e(R/W)}{\pi k L}$$

Although this is a highly idealised case we see already the important conclusion that the temperature rise is not simply a function of the power density but of the power input per unit length. In fact the power density alone is never sufficient to characterise a thermal problem. In the present example we expect heat to flow away from the line of input and cause reasonably large temperature gradients and slope errors in the transverse direection. We would expect to be able to analyse the situation to a good approximation with a two dimensional heat transfer calculation. Conversely in the longitudinal direction if L is very large we expect to see approximately linear heat flow and if the heat load is truly constant along L we expect to see no temperature gradients and no slope errors in that direction, except at the ends. If there were slight departures from the constant value of the heat load along L we expect slope errors given by[45]

$$\text{Slope} = \frac{t^2\alpha}{k}\frac{dD}{dx}$$

i.e. proportional to the derivitive of the power density and to α/k (t is the thickness). k/α is in fact the thermal distortion figure of merit for materials.

We have so far overlooked a possibly important fact: that our slab of material with a temperature difference ΔT across it, may, if it is free enough to move become longer at the top than the bottom by an amount $L\alpha\Delta T$. Therefore, the strain would be $\alpha\Delta T$ and the stress $E\alpha\Delta T$. Obviously we can prevent the mirror bending by suitable stiffening but the mirror material must still be subject to a stress $E\alpha\Delta T$ (or something similar depending on the exact constraints and the Poissons ratio).

Given the great difference in response between the transverse and longitudinal directions we recognise a helpful correspondance with surface tolerances which are often looser (see Section 5.2) in the transverse direction (where slope errors tend to be worse) and tighter in the longitudinal direction where thermal distortion tends to be less. This is based on the idea that the derivitive of the power density is the main driver of slope errors.

Let us consider some magnitudes. Suppose the total power is 7kW. This corresponds to the 54 pole wiggler on SPEAR[46] with parameters set for highest power output. Suppose we remove all of this heat by water flow with a temperature rise of 20°C. The needed flow rate is 5 liters per minute. This is a modest flow rate. Therefore, getting the heat out is not the problem.

Now suppose we have a copper mirror with a ΔT of 100°C. $E\alpha\Delta T$ in this case is 28,400 pounds per square inch. To see if this is in the safe range we show in fig. 6 the fatigue/stress relation for oxygen free copper.[47] We see that for 10^4 or 10^5 cycles which is a reasonable estimate for the lifetime of a synchrotron radiation beamline optic, 28,400 pounds per square inch is not in the safe range and might lead to cracking or some other form of failure.[48]

6.3 Summary on thermal loading

- It is easy to get the heat out and this is not the problem
- Even for moderate ΔT's thermal stresses can be a problem
- The surface slope errors due to thermal distortion are often associated with a large spatial rate of change in the applied power density
- Distortion is minimised by using materials with high k/α
- The best materials from a stress point of view are those with

the highest value of $\sigma_y k/E\alpha$ where σ_y is the 0.1% yield stress

- The objective of design work is to remove the heat in such a way that the stress is in the safe range (achieved by controlling ΔT) and the surface slope errors are within tolerance
- Low values of ΔT are most easily achieved by applying cooling at a distance less than the smallest dimension of the beam footprint

6.4 Computer modelling of thermal loading

In order to calculate the ΔT's, stresses and distortions arising in practical geometries for cooling mirrors it is almost always necessary to use numerical techniques. Since thermal analysis is important in many branches of engineering there is an extensive literature on the subject and universal computer programs are sold commercially by which any chosen geometry can be analysed. These programs use the so called "finite element method" of analysis which is based on the use of a mesh of discrete points to model the system. Information must be provided to define boundary conditions (heat input and output to and from the system at mesh points on the system boundaries) and the program then computes the temperature, stress and displacement at each point in the mesh. Two dimensional finite element calculations are generally quite routine and inexpensive but three dimensional calculations become very expensive if a large number of mesh points are required.

As an example of this technique we show a two dimensional calculation (fig 6) which is taken from the work of DiGennaro.[49]

6.5 Generalised solution of a heated mirror problem

We consider the problem of a heat load which is applied uniformly along the length of a long, narrow mirror. The applied power distribution is approximately Gaussian in the transverse direction with standard deviation $\sigma = bR$. Cooling is provided by a single circular water cooling channel of radius R separated from the mirror surface by a minimum distance aR. The geometry is thus fully characterised by the parameters a and b, R being merely a scale factor. We now conceive some "natural units" for the interesting parameters.

The natural unit for the temperature rise ΔT_{AB} (see fig 7) is ΔT_{lin} which is the temperature rise that would occur between A and B for the power density applied at A, the distance AB and the conductivity of the material in question if the heat flow were linear. The natural unit for the stress is $E\alpha\Delta T_{lin}$ and for the maximum slope error is $\Delta\ell_{AB}/\sigma$ where $\Delta\ell_{AB}$ is the growth in AB that would occur if a length AB were heated by ΔT_{lin} i.e. $\Delta\ell_{AB} = aR\alpha\Delta T_{lin}$ giving $a\alpha\Delta T_{lin}/b$ for the unit of stress. The reason for inventing natural units is so that results can be plotted as universal curves which are good for all materials and power loadings. We give some results of finite element calculations (again from DiGennaro) in fig. 8 presented as universal curves. The assumption in all these calculations is that water flow conditions are the same and correspond to 20ft/sec flow with film coefficient .023 $W/mm^2/°K$. The water/material interface is not taken as isothermal but, rather, realistic calculated values for the heat transfer rates are used.

REFERENCES

1. V. Rehn and V.O. Jones Opt. Eng. 17, 504(1978)
2. V. Rehn SSRL Reports 78/04, VII-1 and 79/02, 153
3. V. Rehn, J.L. Stanford, A.D. Baer, V.O. Jones and W.J. Choyke Appl. Opt. 16, 1111(1977)
4. V. Rehn and W.J. Choyke Nucl. Inst. Meth. 177, 173(1980) and Conference on "Low Energy X-ray Diagnostics" (Monterey 1981), D.T. Attwood and B.L. Henke (eds) AIP #75 p.162
5. R.L. Johnson in "Handbook on Synchrotron Radiation Vol 1A, E-E.Koch (ed), (North Holland, Amsterdam 1983)
6. M.R. Howells, Appl. Opt 19, 4027(1980)
7. R. Zietz and V. Saille, 6th Conference on Vacuum Ultra Violet Radiation Physics, Charlottesville, 1980 paper III-42
8. M.R. Howells (ed), Reflecting Optics for Synchrotron Radiation, Proc. SPIE 315(1981), RAL Symposium on New Techniques in X-ray and XUV Optics, Rutherford Laboratory report RL-83-010 (1982), Workshop on X-ray Instrumentation for Synchrotron Radiation Research, Stanford Synchrotron Radiation Laboratory report 78/04 (1978)

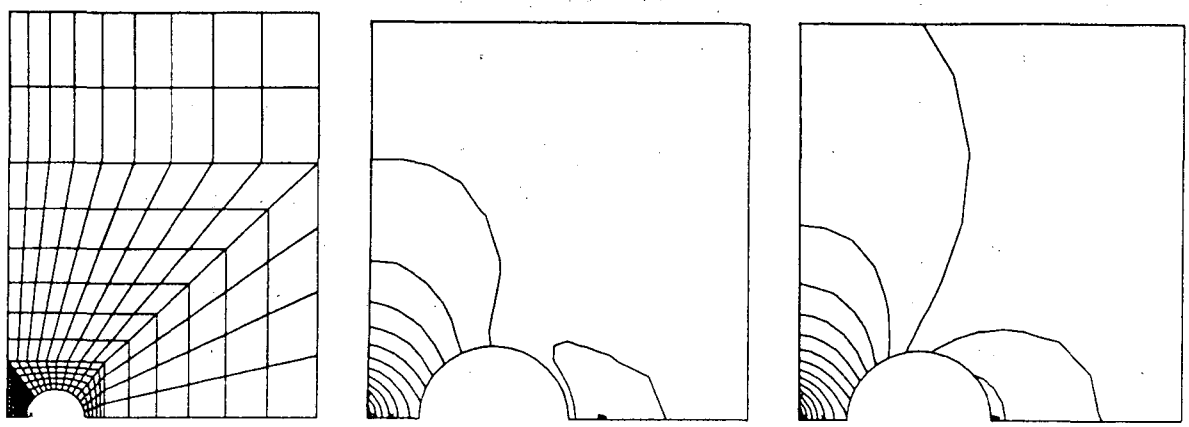

Fig 6. Example of a two dimensional finite element calculation. Left picture shows the mesh of points describing a 6 mm diameter water channel in a copper alloy mirror, at a distance 2 mm from the optical surface. An approximately gaussian power load with σ = .85 mm, peak power density 5 W/mm² is applied symmetrically. Center picture shows the isothermals calculated by the finite element program ANSYS at 2°C intervals. The hottest point on the optical surface is the center point at 72.5°C. The water surface is at 58°C on the hot side, 39°C on the cold. Right hand picture shows the stress contours (Von Mises equivalent) at 4x10⁶ Pa intervals. Maximum stress occurs at the center and is 9.12x10⁷ Pa(≡ 13200 psi), hence the use of the special copper alloy: Glidcop (see reference 49)

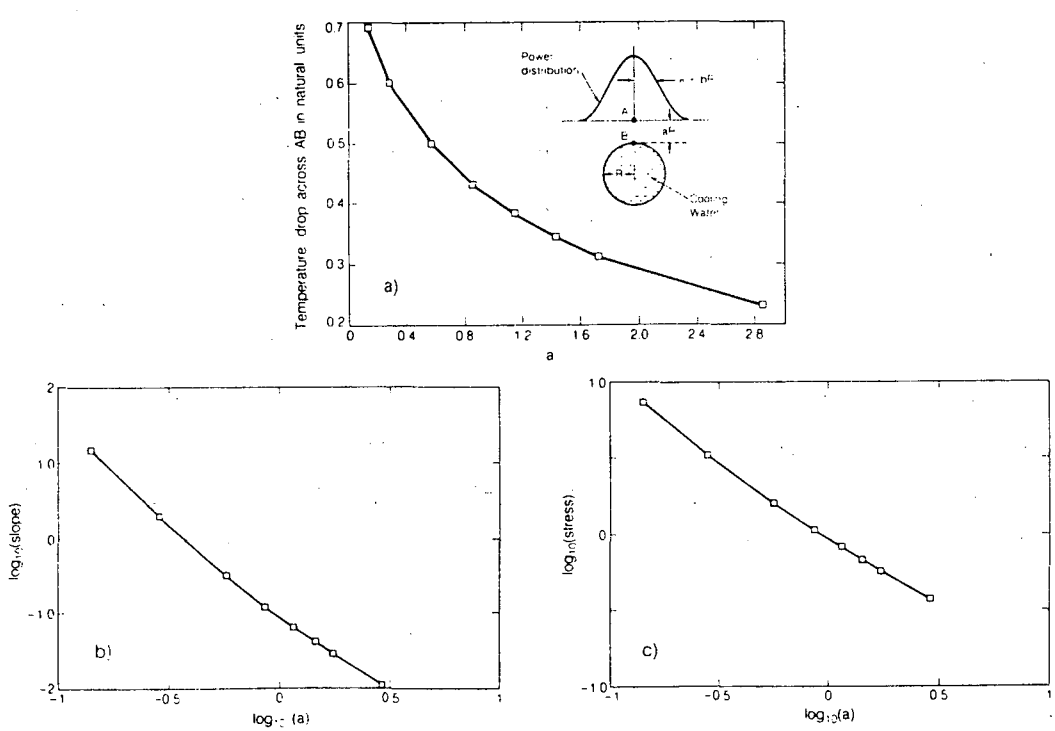

Fig 7. Plots of (a) ΔT_{AB}, (b) maximum slope error and (c) maximum stress as a function of the parameter a with parameter b = 0.243 (see inset diagram). All these quantities are expressed in the natural units defined in the text.

9. Various conferences on synchrotron radiation instrumentation published in Nucl. Inst. Meth: Montpelier 152(1978), Gaithersburg 172(1980), Honolulu 177(1980), Ithaca 195(1982), Hamburg 208(1983) Brookhaven 222(1984)

10. For an excellent overview of X-ray Optics see J.H. Underwood, "X-ray Optics", American Scientist 66, 476(1978)

11. R.C. Chase, G.W. Kuswa (eds) "X-ray Imaging", Proc SPIE 106(1977)

12. M. Weisskopf (ed) "Space Optics" Proc SPIE 184(1979)

13. R. Giacconi and H. Gursky "X-ray Astronomy" (eds), (Reidel, Dordrecht, Holland, 1974)

14. "High power lasers and applications" Proc SPIE 270 and 455

15. "Laser induced damaged in optical materials: 1982" Conference proceedings from Boulder, SP669, Stock #003-003-02563-1 (US government printing office, Washington, 1982)

16. Conference see ref. 4

17. M. Born and E. Wolf, "Principles of Optics", (Pergamon, Oxford, 1983)

18. See reference 17 para 13.4.1 equations 8 and 15 with notation changes $v_2 \to v$, $u_2 \to u$, $\theta_1 \to \theta$, $n_2 \to 1$ $\kappa_1 \to \bar{k}/n$, $\kappa_2 \to 0$, $n_1 \to n$, τ_{12}, χ_{12} are analagous to our ρ and ϕ for the reflection case

19. B.L. Henke, P. Lee, T.J. Tanaka, R.L. Shimabukuro and B.K. Fujiwara, At. Data. Nucl. Data. Tables 27, 1(1982)

20. See refs 3, 4 plus A. Franks and M. Stedman, Nucl. Inst. Meth. 172, 249(1980), P.Z. Takacs Nucl. Inst. Meth. 195, 259(1982) and Brookhaven report BNL 30341

21. There is not much in the literature about low scatter finishing techniques, especially for metals and aspherics since most firms consider them proprietory. R.W. Dietz and J.M. Bennett Appl. Opt. 5, 881(1966) P.C. Baker and N.J. Brown Opt. Eng. 17, 595(1978), S.R. Lange and R.E. Parks Proc. SPIE 257, 169 (1980)

22. A.S. Devaney, "Master Optical Techniques" (Wiley New York, 1981) and G.W. Fynn and W.J.A. Powell "The Cutting and Polishing of Electro-optic Materials (Wiley, New York, 1979)

23. D. Malacara, "Optical Shop Testing" (Wiley, New York, 1978)

24. There are no commercially available instruments for measuring the figure of grazing incidence aspherics. Various laboratory

instruments exist for example: M. Stedman and V.W. Stanley Proc. SPIE 163, 99(1979) J.M. Eastman, J.M. Zavislan Proc. SPIE 429(1983) K. Von Bieren. Appl. Opt. 22, 2109(1983), S. Bernstorff Internal Report DESY F41, HASYLAB 80/01 for reviews see R.H. Price, p.189 in the Conference cited in reference 4 and P.Z. Takacs in Conference cited in reference 43

25. It is routine to get spherical optics with surfaces spherical within $\lambda/20$ (λ = 6328Å). Considering the method of manufacture this should give slope errors of about $\lambda/20$ divided by half of the width. Better tolerances than $\lambda/20$ can be achieved. $\lambda/40$ is quite common. The limit may be around $\lambda/100$
26. See for example J.H. Underwood, Space Sci. Inst. 3, 259(1977), J.H. Underwood and D. Turner ref. 11, J.A. Howell, Ph.D. Thesis, Harvard University 1974, S. Heald and J. Hastings, Nucl. Inst. Meth. 187, 553(1981)
27. "Adaptive Optics", proc. SPIE volumes 141, 179, 365 and 551
28. See for example ref 5 and H. Noda, T. Namioka and M. Seya J. Opt. Soc. Am. 64, 1031(1974)
29. Ref. 5 and S.O. Kastner and W.M. Neupert, J. Opt. Soc. Am. 53, 1180(1963), G.H. Spencer and M.V.R.K. Murty J. Opt. Soc. Am. 52, 672(1962), F. Cerrina Proc. SPIE 503, 68(1984). There are many commercially available ray trace programs intended for lens design that are difficult to adapt to beamline needs. The only general purpose program directed toward synchrotron radiation applications seems to be F. Cerrina's SHADOW
30. See for example E.L. Church and P.Z. Takacs proc. SPIE 508, 105(1985), E.L. Church Proc. SPIE 429, 86 and 105(1983)
31. E.L. Church, H. Jenkinson and J.M. Zavada, Opt. Eng. 18, 125(1979)
32. E.L. Church, M.R. Howells and T.V. Vorburger Proc. SPIE 315, 202(1981)
33. From the definition of the autocovariance function one can see that σ^2 is the autocovariance function at zero lag. By the Weiner-Khintchine Theorem the latter function is given by the Fourier Transform of the power spectrum so writing this down and

setting the lag equal to zero we find that σ^2 is simply an integral over the power spectrum from f_{min} to f_{max} (also called the zeroth moment of the power spectrum), see reference 31

34. Instruments supplied by WYKO Corp. 2990, E. Ft. Lowell, Tucson, Az. 85716
35. Data supplied by P.Z. Takacs and J. Colbert of Brookhaven National Laboratory
36. m is given by the second moment of the power spectrum see reference 31
37. D.A. Shirley, SSRL report 78/04(1978)
38. K. Boller, R.P. Haelbich, H. Hogrefe, W. Jark and C. Kunz DESY report SR-82-18(1982)
39. T. Koide et al KEK preprint 85-35(1985)
40. W.R. McKinney and P.Z. Takacs Nucl. Inst. Meth. 195, 371(1982)
41. W.D. Beverley, R.B. Gillette and G.A. Cruz in Thermal Control and Radiation, AIAA progress Series, Chang-Lin Tien (ed) (MIT Press, Cambridge, 1973) Vol 31, p159
42. A. Franks and M. Stedman Nucl. Inst. Meth 172, 249(1980)
43. K.J. Kim, Conference on Synchrotron Radiation Instrumentation, Stanford, 1985 to be published in Nucl. Inst. Meth.
44. G.K. Green, Brookhaven Laboratory Report BNL 50595 Vol II, equation 87
45. For nearly linear heat flow we can think of the block as composed of "columns" each expanding according to its own ΔT. Thus $y = t(1+\alpha\Delta T)$ and $dy/dx = t\alpha d(\Delta T)/dx$. For each column of area A, $DA = kA\Delta T/t$. Combining these equations leads to the one given
46. C. Bahr et al, Nucl. Inst. Meth. 208, 117(1983)
47. S. Sharma and S. Ulc, in "NSLS Superconducting Wiggler beamline (X17) Conceptual Design Report" W. Thomlinson (ed) Brookhaven Report March 1984
48. A.A. Macdowell and J.B. West loc. cit. ref. 43
49. R. DiGennaro Lawrence Berkeley Laboratory preprint LBL-20468, Conference on Insertion Devices for Synchrotron Sources, Stanford, 1985 to be published in Proc. SPIE
50. R. Avery, Nucl. Inst. Meth. 222, 146(1984)

This report was done with support from the Department of Energy. Any conclusions or opinions expressed in this report represent solely those of the author(s) and not necessarily those of The Regents of the University of California, the Lawrence Berkeley Laboratory or the Department of Energy.

Reference to a company or product name does not imply approval or recommendation of the product by the University of California or the U.S. Department of Energy to the exclusion of others that may be suitable.

LAWRENCE BERKELEY LABORATORY
TECHNICAL INFORMATION DEPARTMENT
UNIVERSITY OF CALIFORNIA
BERKELEY, CALIFORNIA 94720